PCCP

SAFT-VR modelling of the phase equilibrium of long-chain n-alkanes

Clare McCabe[a] and George Jackson[b]

[a] *Department of Chemistry, University of Sheffield, Sheffield, UK S3 7HF*
[b] *Department of Chemical Engineering and Chemical Technology, Imperial College of Science, Technology and Medicine, Prince Consort Road, London, UK SW7 2BY*

Received 19th October 1998, Accepted 3rd December 1998

The statistical associating fluid theory for potentials of variable attractive range (SAFT-VR) has been used in the calculation of the phase equilibria for long-chain n-alkanes and their mixtures. We treat the molecules as chains formed from united-atom hard-sphere segments, with a square-well potential of variable attractive range to describe the dispersive forces. A empirical relationship derived in earlier work is used to determine the number of such segments in relation to the carbon number for each member of the homologous series. Simple linear relationships between the potential model parameters and molecular weight have been determined enabling predictions of the fluid phase equilibria of heavier n-alkane molecules for which no experimental data are available. This is illustrated by a comparison with simulation data from the literature for the coexisting densities of n-octatetracontane ($C_{48}H_{98}$). Additionally we have examined binary mixtures of methane + n-hexadecane ($C_{16}H_{34}$) and hexane + n-tetradecane ($C_{14}H_{30}$) with the SAFT-VR approach, using simple Lorentz–Berthelot combining rules to determine the unlike interaction parameters. This study will allow an extension of the SAFT-VR approach to polymeric systems.

1 Introduction

A knowledge of the thermodynamics and phase behaviour of fluid systems is central to chemical process design in the traditional chemical and oil industries, for example in supercritical fluid extraction, chromatography, surfactancy and the development of separation and extraction processes.[1,2] The thermophysical properties of hydrocarbon compounds in particular are of increasing importance to the petroleum industry, from the manufacture of waxes and polymers to enhanced oil recovery and as model compounds in the development and testing of correlations for predicting the properties of petroleum fractions.[3]

Experimental measurements on the thermodynamic properties of n-alkanes have been under way for over 100 years, with reviews of vapour-pressure data dating back as early as 1882.[4] While accurate experimental results of the thermodynamic properties of light hydrocarbons over the whole phase diagram are readily available,[5–7] those of heavier hydrocarbons are somewhat patchy and less reliable. Hydrocarbons are thermally unstable at temperatures above 650 K making experimental investigation on n-alkanes heavier than decane ($C_{10}H_{22}$) difficult.[8] Experimental results for the vapour-pressure curves of n-alkanes up to hexatriacontane ($C_{36}H_{74}$) are available.[9–11] Unfortunately, these early measurements on heavier n-alkanes suffered from problems of impurity, dissolved gases and decomposition, and a wide scatter is observed between different sets of experimental results. It is only more recently with the development of new experimental techniques that vapour-pressure and critical data for the longer n-alkanes have been measured accurately.[12–15]

In order to create a complete picture of the thermodynamic properties of hydrocarbons, and fluids in general, several theoretical methods have been developed to extrapolate existing experimental data and provide predictions of the thermodynamic properties for which experimental results are not available. There are numerous theoretical approaches in the literature which generally fall into one of three classes: empirical correlations, corresponding states theories and equations of state.

Equations of state have been used by researchers in the study of vapour pressures and other thermophysical properties since the time of van der Waals. Although the cubic equations of state based on the van der Waals equation, namely Redlich–Kwong (RK),[16] Soave–Redlich–Kwong (SRK)[17] and Peng–Robinson (PR),[18] have been used to examine the phase behaviour of n-alkanes they tend to give poor results for the longer n-alkane chains, as they do not take into account the non-sphericity of the fluid.[19–21] The perturbed hard chain theory (PHCT) proposed in the late 1970s by Prausnitz and co-workers[22] was one of the first equations to treat the chain nature of molecules. The PHCT equation was fitted to the vapour-pressure curves of n-alkanes from methane to n-eicosane ($C_{20}H_{42}$) giving correlations of the model parameters enabling estimates to be made for other members of the homologous series for which no experimental data were available. The simplified perturbed hard chain theory (SPHCT) was proposed by Kim *et al.*[19] and used to predict the vapour pressures and saturated liquid densities of n-alkanes, again up to n-eicosane. Though larger errors were seen for the liquid densities of the hydrocarbons than with the original PHCT equation, the correlations for the n-alkane parameters from SPHCT were successfully used and extrapolated to n-tetracosane ($C_{24}H_{50}$) in the study of ethane + n-alkane binary mixtures by Peters *et al.*[23] Later, attempts by Gasem and Robinson[21] to use the correlations of Kim *et al.*[19] produced poor results for heavier hydrocarbons and so new correlations for the pure component parameters of n-alkanes from methane to n-tetrahexacontane ($C_{64}H_{130}$) were obtained. While a reasonable representation of both the vapour pressures and liquid densities of the n-alkanes was obtained from this work, errors were seen near the critical point (a feature of all such analytical equations of state) and the triple point, which were probably due to fitting the parameters to only a limited range of state points.

The statistical associating fluid theory (SAFT) was orig-

inally developed[24,25] to model associating fluids as chains of Lennard-Jones segments with association sites. There have been many variations on the original theory since its introduction in the late 1980s (see ref. 26 for recent overview). In its various forms SAFT has been used extensively to correlate and predict experimental results of a wide variety of substances and their mixtures. For example Huang and Radosz[27,28] correlated the data for over 100 real fluids including 17 n-alkanes from methane to n-tetratetracontane ($C_{44}H_{90}$). Blas and Vega[29] have proposed a version of SAFT based on an extension of Wertheim's theory for Lennard-Jones fluids due to Johnson *et al.*[30] They obtain excellent results for the phase equilibrium of binary and ternary mixtures of low molecular weight n-alkanes, alkenes and alcohols. While the expressions of Johnson *et al.* give an accurate representation of the Lennard-Jones fluid the expression is described by 32 constants. The SAFT-VR approach[26,31] is a recent extension of the SAFT theory for potentials of variable attractive range. SAFT-VR can be applied to soft potentials, requiring only 12 constants, as presented in the original paper[26] where a comparison was made with the expressions of Johnson *et al.* and comparable accuracy seen away from the critical region. Furthermore the same 12 constants in SAFT-VR are applicable to variable ranges of the potential. In this work we use a version of the statistical associating fluid theory (SAFT-VR) to predict the vapour pressures and saturated liquid densities of long-chain n-alkanes. We extend the scope of the original work on n-alkanes from methane to n-octane,[26] to n-hexatriacontane ($C_{36}H_{74}$) and obtain correlations of the model parameters to enable extrapolation to longer members of the homologous series. The approach has been applied to a variety of industrially important systems, *e.g.* n-alkanes (from methane to n-octane), perfluoro-n-alkanes and their mixtures,[26,32–34] refrigerant systems,[35] hydrogen chloride + n-alkanes,[36] *etc.* Here we extend the scope of the original work on the n-alkanes to higher chain lengths, obtaining excellent agreement between SAFT-VR predictions and the experimental or pseudo-experimental data[37] for both the vapour-pressure curves and saturated liquid densities. We observe a linear relation for the pure component parameters with molecular weight. This enables prescriptions to be determined from which we can obtain the parameters for heavier hydrocarbons. Additionally we examine the binary mixtures of methane + hexadecane ($C_{16}H_{34}$) and hexane + n-tetradecane ($C_{14}H_{30}$), further illustrating the applicability of the SAFT-VR approach to heavier n-alkanes. The unlike model parameters required for the description of binary phase behaviour with the SAFT-VR approach are obtained from those of the pure components, by using Lorentz–Berthelot combining rules as in earlier work.[32,33] For the methane + hexadecane system Peters and co-workers[38,39] have measured the low temperature region of the phase diagram, though we have concentrated on the high temperature results of Lin *et al.*[40] in order to compare the SAFT-VR predictions with both best-fitted and re-scaled parameters in the critical region.

2 Models and theory

The n-alkane molecules are described as a simple united-atom model: m hard-spherical segments of diameter σ tangentially bonded together to form chains. The attractive interactions are modelled with a square-well potential of variable width λ and depth ε:

$$u(r) = \begin{cases} +\infty & \text{if } r < \sigma \\ -\varepsilon & \text{if } \sigma \leqslant r < \lambda\sigma \\ 0 & \text{if } r \geqslant \lambda\sigma \end{cases} \quad (1)$$

A simple empirical relationship[41,42] is used to determine the number of such segments in relation to the number of carbon atoms C [$m = \frac{1}{3}(C-1)+1$], hence for methane $m = 1$, ethane $m = 1.33$, propane $m = 1.67$, *etc.* This relationship gives a reasonable description of the critical temperatures and pressures of the homologous series of n-alkanes; however it is too simplistic to reproduce the finer details, such as the anomalously low critical pressure of methane.[43]

In this paper we will only summarise the main expressions of the SAFT-VR theory for the square-well potential; the reader should consult refs. 26 and 31 for details. The general equation for mixtures of chain molecules formed from hard-core segments with attractive interactions is given followed by the specific expressions for a binary mixture. The Helmholtz free energy A for an n-component mixture of chain molecules can be separated into the various contributions as

$$\frac{A}{NkT} = \frac{A^{\text{IDEAL}}}{NkT} + \frac{A^{\text{MONO.}}}{NkT} + \frac{A^{\text{CHAIN}}}{NkT} \quad (2)$$

where N is the total number of molecules, T is the temperature and k is the Boltzmann constant. There is no need to include the association term since we are dealing with non-associating n-alkane systems. The ideal contribution to the free energy is given by a sum over all species i in the mixture,[44]

$$\frac{A^{\text{IDEAL}}}{NkT} = \left(\sum_{i=1}^{n} x_i \ln \rho_i \Lambda_i^3\right) - 1 = x_1 \ln \rho_1 \Lambda_1^3 + x_2 \ln \rho_2 \Lambda_2^3 - 1 \quad (3)$$

where $x_i = N_i/N$ is the mole fraction, $\rho_i = N_i/V$ the molecular number density, N_i the number of molecules, Λ_i the thermal de Broglie wavelength of species i and V the volume of the system. We can express the monomer Helmholtz free energy by

$$\frac{A^{\text{MONO.}}}{NkT} = \left(\sum_{i=1} x_i m_i\right)\frac{A^M}{N_s kT} = \left(\sum_{i=1} x_i m_i\right)a^{\text{M}} = (x_1 m_1 + x_2 m_2)a^{\text{M}} \quad (4)$$

where m_i is the number of spherical segments of chain i.

Using the Barker and Henderson high temperature perturbation theory[45] for mixtures with a hard-sphere reference system, the monomer free energy per segment of the mixture is obtained from the expansion,

$$a^{\text{M}} = a^{\text{HS}} + \beta a_1 + \beta^2 a_2 \quad (5)$$

where $\beta = 1/kT$ and each term is now for a mixture of spherical segments. The expression of Boublik[46] and Mansoori *et al.*[47] for a multi-component mixture of hard spheres is used for the reference hard-sphere term,

$$a^{\text{HS}} = \frac{6}{\pi\rho_s}\left[\left(\frac{\zeta_2^3}{\zeta_3^2} - \zeta_0\right)\ln(1-\zeta_3) + \frac{3\zeta_1\zeta_2}{(1-\zeta_3)} + \frac{\zeta_2^3}{\zeta_3(1-\zeta_3)^2}\right] \quad (6)$$

where ρ_s is the total number density of spherical segments and ζ_l are the reduced densities defined by

$$\zeta_l = \frac{\pi\rho_s}{6}\left[\sum_{i=1}^{n} x_{s,i}\sigma_{ii}^l\right] = \frac{\pi\rho_s}{6}\left[x_{s,1}\sigma_{11}^l + x_{s,2}\sigma_{22}^l\right] \quad (7)$$

Here σ_{ii} is the diameter of the spherical segments of chain i, and $x_{s,i}$ is the mole fraction of segments of type i in the mixture.

The mean-attractive energy represented by the a_1 term is obtained from the sum of the partial terms corresponding to each type of pair interaction,[26,31]

$$a_1 = \sum_{i=1}^{n}\sum_{j=1}^{n} x_{s,i}x_{s,j}a_1^{ij} = x_{s,1}^2 a_1^{11} + 2x_{s,1}x_{s,2}a_1^{12} + x_{s,2}^2 a_1^{22} \quad (8)$$

where

$$a_1^{ij} = -2\pi\rho_s\varepsilon_{ij}\int_{\sigma_{ij}}^{\infty} r_{ij}^2 g_{ij}^{HS}[r_{ij};\zeta_3]\,dr_{ij} \quad (9)$$

and g_{ij}^{HS} is the radial distribution function for a mixture of hard spheres. Using the mean-value theorem[26,31] we obtain an expression for a_1 in terms of the contact value of g_{ij}^{HS}:

$$a_1 = -\rho_s\sum_i\sum_j x_{s,i}x_{s,j}\alpha_{ij}^{VDW}g_{ij}^{HS}[\sigma_{ij};\zeta_3^{eff}] \quad (10)$$

where

$$\alpha_{ij}^{VDW} = 2\pi\varepsilon_{ij}\sigma_{ij}^3(\lambda_{ij}^3 - 1)/3 \quad (11)$$

is the van der Waals attractive constant for the i–j interaction, and ζ_3^{eff} is an effective packing fraction.

In the van der Waals one (VDW-1) fluid theory g_{ij}^{HS} is approximated by the radial distribution function for a single fluid so that eqn. (10) simplifies to

$$a_1 = -\rho_s\sum_i\sum_j x_{s,i}x_{s,j}\alpha_{ij}^{VDW}g_0^{HS}[\sigma_x;\zeta_x^{eff}] \quad (12)$$

where g_0^{HS} is the contact value of the hard-sphere pair radial distribution obtained from the Carnahan and Starling equation of state,[48]

$$g_0^{HS}[\sigma_x;\zeta_x^{eff}] = \frac{1-\zeta_x^{eff}/2}{(1-\zeta_x^{eff})^3} \quad (13)$$

The effective packing fraction ζ_x^{eff} in eqn. (13) is obtained within the VDW-1 fluid approximation from the corresponding packing fraction of the mixture, ζ_x :

$$\zeta_x^{eff}(\zeta_x,\lambda_{ij}) = c_1(\lambda_{ij})\zeta_x + c_2(\lambda_{ij})\zeta_x^2 + c_3(\lambda_{ij})\zeta_x^3 \quad (14)$$

where

$$\zeta_x = \frac{\pi}{6}\rho_s\sum_i\sum_j x_{s,i}x_{s,j}\sigma_{ij}^3 = \frac{\pi}{6}\rho_s\sigma_x^3 \quad (15)$$

with

$$\sigma_x^3 = \sum_i\sum_j x_{s,i}x_{s,j}\sigma_{ij}^3 \quad (16)$$

The coefficients c_1, c_2 and c_3 are approximated by those of the pure fluid,[26–31]

$$\begin{pmatrix}c_1\\c_2\\c_3\end{pmatrix} = \begin{pmatrix}2.25855 & -1.50349 & 0.249434\\ -0.669270 & 1.40049 & -0.827739\\ 10.1576 & -15.0427 & 5.30827\end{pmatrix}\begin{pmatrix}1\\\lambda_{ij}\\\lambda_{ij}^2\end{pmatrix}. \quad (17)$$

This corresponds to the MX1b mixing rule of ref. 31. The MX1b prescription gives a consistent representation of both vapour–liquid and liquid–liquid critical behaviour.[33] If the actual packing fraction ζ_3 of the system is used in order to get ζ_3^{eff} according to the mapping rule for pure components (MX3b mixing rule in ref. 31) there are some problems associated with the critical region of the phase diagram. This is a common feature of equations of state for mixtures which use parameters defined for pure fluids beyond the VDW-1 fluid approximation.[49–50]

The first fluctuation term a_2 is given by[26,31]

$$a_2 = \sum_{i=1}^{n}\sum_{j=1}^{n} x_{s,i}x_{s,j}a_2^{ij} = x_{s,1}^2 a_2^{11} + 2x_{s,1}x_{s,2}a_2^{12} + x_{s,2}^2 a_2^{22} \quad (18)$$

The terms a_2^{ij} are obtained from the expressions for a_{ij} with the local compressibility approximation,[51]

$$a_2^{ij} = \frac{1}{2}K^{HS}\varepsilon_{ij}\rho_s\frac{\partial a_1^{ij}}{\partial\rho_s} \quad (19)$$

where K^{HS} is the hard-sphere isothermal compressibility of Percus and Yevick,[52]

$$K^{HS} = \frac{\zeta_0(1-\zeta_3)^4}{\zeta_0(1-\zeta_3)^2 + 6\zeta_1\zeta_2(1-\zeta_3) + 9\zeta_2^3} \quad (20)$$

Finally, the contribution to the free energy due to chain formation is expressed in terms of the contact value of the background correlation function,[26,31]

$$\frac{A^{CHAIN}}{NkT} = -\sum_{i=1}^{n} x_i(m_i-1)\ln y_{ii}^{SW}(\sigma_{ii}) = -x_1(m_1-1)\ln y_{11}^{SW}(\sigma_{11}) - x_2(m_2-1)\ln y_{22}^{SW}(\sigma_{22}) \quad (21)$$

where $y_{ii}^{SW}(\sigma_{ii}) = g_{ii}^{SW}(\sigma_{ii})\exp(-\beta\varepsilon_{ii})$. We obtain $y_{ii}^{SW}(\sigma_{ii})$ from the high-temperature expansion of $g_{ii}^{SW}(\sigma_{ii})$,

$$g_{ii}^{SW}(\sigma_{ii}) = g_{ii}^{HS}(\sigma_{ii}) + \beta\varepsilon_{ii}g_1(\sigma_{ii}) \quad (22)$$

The hard-sphere term g_{ii}^{HS} is given by the expression of Boublik,[46]

$$g_{ij}^{HS}(\sigma_{ij};\zeta_3) = \frac{1}{1-\zeta_3} + 3\frac{D_{ij}\zeta_3}{(1-\zeta_3)^2} + 2\frac{(D_{ij}\zeta_3)^2}{(1-\zeta_3)^3} \quad (23)$$

with the parameter D_{ij} defined by

$$D_{ij} = \frac{\sigma_{ii}\sigma_{jj}}{\sigma_{ii}+\sigma_{jj}}\frac{\sum_{i=1}^{n}x_{s,i}\sigma_{ii}^2}{\sum_{i=1}^{n}x_{s,i}\sigma_{ii}^3} \quad (24)$$

The term $g_1(\sigma_{ii})$ is obtained from a self-consistent representation of the pressure P from the Clausius virial theorem and from the density derivative of the Helmholtz free energy,[26,31]

$$g_1[\sigma_{ii};\zeta_3] = g_0^{HS}[\sigma_x;\zeta_x^{eff}] + (\lambda_{ii}^3-1)\frac{\partial g_0^{HS}[\sigma_x;\zeta_x^{eff}]}{\partial\zeta_x^{eff}} \times\left(\frac{\lambda_{ii}}{3}\frac{\partial\zeta_x^{eff}}{\partial\lambda_{ii}} - \zeta_3\frac{\partial\zeta_x^{eff}}{\partial\zeta_3}\right) \quad (25)$$

This corresponds to the MX1b mixing rule of ref. 31 where a VDW-1 representation of g_0^{HS} is used; note that the full g^{HS} reference is used in the first term of eqn. (22).

Using standard relationships other thermodynamic properties can be obtained from the Helmholtz free energy. The chemical potential is given by

$$\mu_i = \left(\frac{\partial A}{\partial N_i}\right)_{T,V,N_{j\neq i}} \quad (26)$$

and the compressibility factor by

$$Z = \frac{pV}{NkT} = \sum_i^n\left(x_i\frac{\mu_i}{kT}\right) - \frac{A}{NkT} \quad (27)$$

These are the functions required for the determination of the critical and phase behaviour of the mixture. The gas–liquid

and liquid–liquid critical lines can be determined by equating to zero the second and third derivatives of the Gibbs free energy with respect to the mole fraction. Phase equilibria between phases I and II in mixtures require that the temperature, pressure, and chemical potential of each component in each phase be equal,[49]

$$T^{I} = T^{II}, \qquad p^{I} = p^{II}, \qquad \mu_i^{I} = \mu_i^{II} \tag{28}$$

These conditions are solved numerically using a simplex method.[53]

3 Results

The SAFT-VR description of the phase equilibria of the n-alkanes, n-nonane (C_9H_{20}) to n-eicosane ($C_{20}H_{42}$), n-tetracosane ($C_{24}H_{50}$), n-octacosane ($C_{28}H_{58}$), n-dotriacontane ($C_{32}H_{66}$), and n-hexatriacontane ($C_{36}H_{74}$), is obtained. The results of the SAFT-VR equation of state for each n-alkane molecule studied are compared with correlated data[37] rather than experimental data as this provides a more complete description of the fluid region; from a comparison of the correlated data with the available experimental data (*e.g.* refs. 5, 12–14) no significant deviations were observed. The model parameters (σ, ε and λ) required to describe the phase equilibria of the pure components with SAFT-VR are obtained by fitting to vapour-pressure and saturated liquid density data from the triple to the critical point using a simplex method.[53] The parameters obtained for n-nonane to n-hexatriacontane are presented in Table 1 as well as those of methane to n-octane from the original work with SAFT-VR.[26] In Fig. 1 we present the SAFT-VR prediction for the vapour pressures of selected n-alkanes and compare the results with correlated vapour-pressure data.[37] This provides a test of the ability of the SAFT-VR approach to describe the phase equilibrium of real chain molecules. From Fig. 1(b) it can be seen that the theory provides a good description of the vapour pressures at low temperatures over the wide range of chain lengths presented, though the agreement is not as good close to the critical point for the longer chain lengths [see Fig. 1(a)], which may be due to poor experimental data given the thermal decomposition of these heavier n-alkanes. SAFT-VR also provides an accurate description of the coexisting densities of the n-alkanes studied, which can be seen in Fig. 2 where we compare SAFT-VR predictions with the correlated data. It is evident from Figs. 1 and 2 that the SAFT-VR approach provides a good description of the phase behaviour of the n-alkanes although the theory over-predicts the critical temperature, and therefore the critical pressure. This is a feature common to all analytical equations of state,[49,54] although if one is interested in critical behaviour it can be avoided by re-scaling the model parameters with respect to

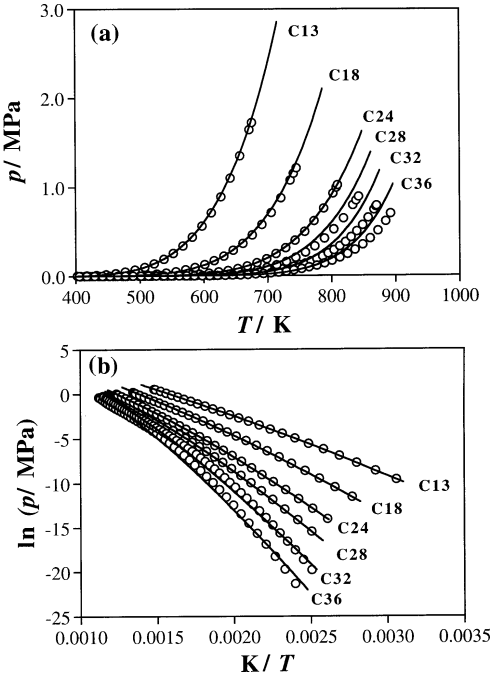

Fig. 1 Vapour pressures for n-tridecane ($C_{13}H_{28}$), n-octadecane ($C_{18}H_{38}$), n-tetracosane ($C_{24}H_{50}$), n-octacosane ($C_{28}H_{58}$), n-dotriacontane ($C_{32}H_{66}$), and n-hexatriacontane ($C_{36}H_{74}$) compared with the SAFT-VR predictions. The circles represent the correlated data[37] and the continuous curves the SAFT-VR results. In (a) we show the vapour-pressure curve as a *p vs. T* representation, and in (b) as a Clausius–Clapeyron plot.

Table 1 Optimised SAFT-VR square-well intermolecular potential parameters for n-alkanes[a]

Substance	m	λ	σ/Å	(ε/k)/K	σ_c/Å	(ε_c/k)/K	T_c^*	P_c^*
CH_4	1.00	1.444	3.670	168.8	4.069	157.4	0.1503	0.009 259
C_2H_6	1.33	1.449	3.788	241.8	4.233	224.8	0.1665	0.007 651
C_3H_8	1.67	1.452	3.873	261.9	4.363	249.3	0.1799	0.006 524
C_4H_{10}	2.00	1.501	3.887	256.3	4.395	243.1	0.1835	0.005 274
C_5H_{12}	2.33	1.505	3.931	265.0	4.475	252.7	0.1927	0.004 700
C_6H_{14}	2.67	1.552	3.920	250.4	4.479	236.6	0.1957	0.003 995
C_7H_{16}	3.00	1.563	3.933	251.3	4.529	237.3	0.2021	0.003 607
C_8H_{18}	3.33	1.574	3.945	250.3	4.564	236.5	0.2076	0.003 275
C_9H_{20}	3.67	1.602	3.938	241.3	4.545	227.4	0.2107	0.002 904
$C_{10}H_{22}$	4.00	1.621	3.959	227.3	4.561	220.4	0.2150	0.002 656
$C_{11}H_{24}$	4.33	1.570	3.973	259.7	4.641	248.8	0.2228	0.002 581
$C_{12}H_{26}$	4.67	1.587	3.953	253.3	4.649	242.3	0.2269	0.002 396
$C_{13}H_{28}$	5.00	1.646	3.950	228.2	4.584	215.4	0.2265	0.002 100
$C_{14}H_{30}$	5.33	1.598	3.961	251.9	4.650	240.6	0.2336	0.002 086
$C_{15}H_{32}$	5.67	1.599	3.991	252.1	4.659	241.3	0.2369	0.001 954
$C_{16}H_{34}$	6.00	1.616	3.980	244.4	4.693	234.6	0.2390	0.001 821
$C_{17}H_{36}$	6.33	1.588	3.997	260.7	4.740	250.7	0.2435	0.001 766
$C_{18}H_{38}$	6.67	1.653	3.941	230.2	4.719	218.1	0.2429	0.001 508
$C_{19}H_{40}$	7.00	1.646	3.964	232.9	4.785	222.3	0.2458	0.001 484
$C_{20}H_{42}$	7.33	1.650	3.966	232.7	4.824	221.5	0.2476	0.001 432
$C_{24}H_{50}$	8.67	1.649	3.972	234.1	4.600	226.5	0.2566	0.001 193
$C_{28}H_{58}$	10.00	1.647	3.980	235.9	4.591	217.8	0.2635	0.001 016
$C_{32}H_{68}$	11.33	1.581	4.026	274.1	4.608	272.6	0.2708	0.000 908
$C_{36}H_{74}$	12.67	1.565	4.037	286.8	4.573	286.0	0.2756	0.000 789

[a] m is the number of spherical segments in the model, λ the range parameter, σ the diameter of each segment, and ε the well depth. The subscript c indicates those parameters that have been re-scaled to the critical point of each pure component. $T_c^* = kT_c b/\alpha$ and $P_c^* = P_c b^2/\alpha$ are the reduced critical temperature and pressure, where $\alpha = 4b\varepsilon(\lambda^3 - 1)$ and $b = \pi\sigma^3/6$

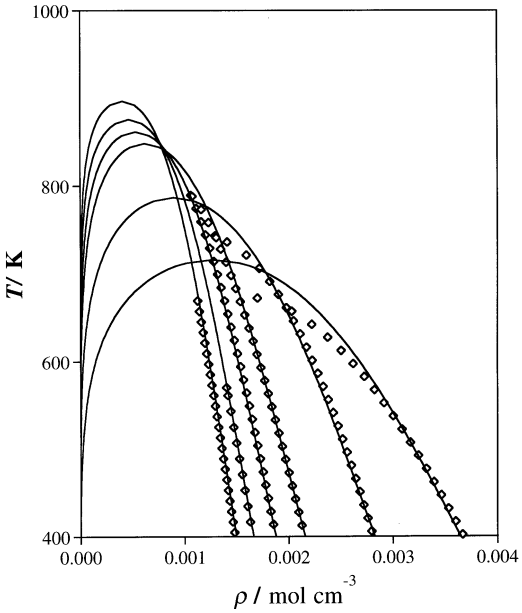

Fig. 2 Coexisting densities for n-tridecane ($C_{13}H_{28}$), n-octadecane ($C_{18}H_{38}$), n-tetracosane ($C_{24}H_{50}$), n-octacosane ($C_{28}H_{58}$), n-dotriacontane ($C_{32}H_{66}$), and n-hexatriacontane ($C_{36}H_{74}$) compared with the SAFT-VR predictions. The diamonds represent the correlated data[37] and the continuous curves the SAFT-VR results.

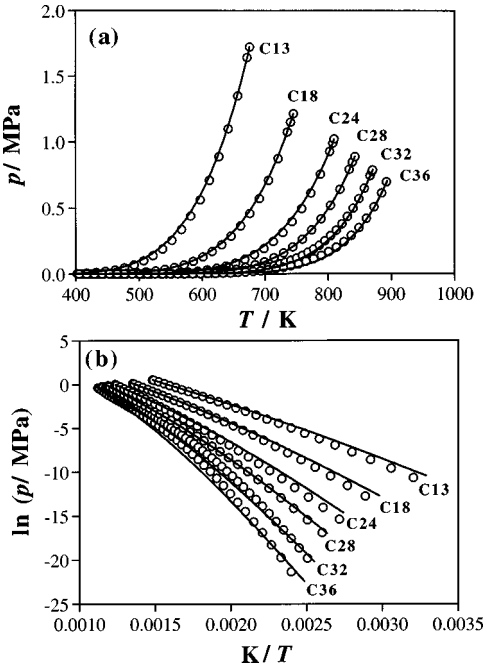

Fig. 3 Vapour pressures for n-tridecane ($C_{13}H_{28}$), n-octadecane ($C_{18}H_{38}$), n-tetracosane ($C_{24}H_{50}$), n-octacosane ($C_{28}H_{58}$), n-dotriacontane ($C_{32}H_{66}$), and n-hexatriacontane ($C_{36}H_{74}$) (from inner curves to the outer) compared with the SAFT-VR prediction using parameters re-scaled to the critical point. The circles represent the correlated data[37] and the continuous curves the SAFT-VR results. In (a) we show the vapour-pressure curve as a *p vs. T* representation, and in (b) as a Clausius–Clapeyron plot.

the pure component experimental critical point. However it should be noted that such re-scaling is at the cost of poorer agreement with the coexisting densities and vapour pressures for temperatures removed from the critical region. The parameters for methane to n-hexatriacontane ($C_{36}H_{74}$) have been re-scaled to the critical point; these are presented in Table 1, as indicated by a subscript c in the column headings. The vapour pressures of the selected n-alkanes obtained from SAFT-VR predictions with the re-scaled parameters are compared with the correlated data in Fig. 3. The SAFT-VR approach with the re-scaled parameters is seen to describe accurately the vapour pressures of the selected n-alkanes, especially in the critical region and with only a slight deviation at lower temperatures.

The parameters for each n-alkane obtained by fitting to vapour-pressure and saturated liquid density data can be depicted graphically as a function of molecular weight (M_r) (Fig. 4). When weighted with the chain length m each parameter is seen to vary linearly with the molecular weight of the n-alkane molecules yielding simple linear relationships:

$$m\lambda = 0.03900M_r + 0.8730 \quad (29)$$

$$m\sigma^3 = 1.566M_r + 24.02 \quad (30)$$

$$m(\varepsilon/k) = 6.343M_r + 76.38 \quad (31)$$

Similar expressions were obtained for the n-alkanes by Vega *et al.*,[29] though only selected n-alkanes from methane to n-octane were studied. Eqns. (29) to (31) provide a means of obtaining parameters for higher members of the n-alkane homologous series for which no experimental data exist. In order to determine the validity of such a procedure a comparison can be made between the SAFT-VR predictions obtained with parameters from the linear prescriptions and results of computer simulation studies of phase equilibrium for heavy n-alkanes.

The development of computer simulation techniques which enable the direct simulation of phase equilibria,[55] and in particular that of chain molecules,[56] has led to a number of workers studying n-alkanes by molecular simulation (see ref. 57 for an overview). Smit and co-workers[57–58] have carried out configurational biased Gibbs ensemble Monte Carlo simulations on n-alkanes from n-pentane (C_5H_{12}) to n-decane ($C_{10}H_{22}$), as well as n-dodecane ($C_{12}H_{26}$), n-hexadecane ($C_{16}H_{34}$), n-tetracosane ($C_{24}H_{50}$) and n-octatetracontane ($C_{48}H_{98}$). Their results are in good overall agreement with the experimental data, and provide predictions for the saturated gas and liquid densities of n-tetracosane and n-octatetracontane for which no experimental data are available. We compare these so called pseudo-experimental data for n-hexadecane, n-tetracosane, and n-octatetracontane with

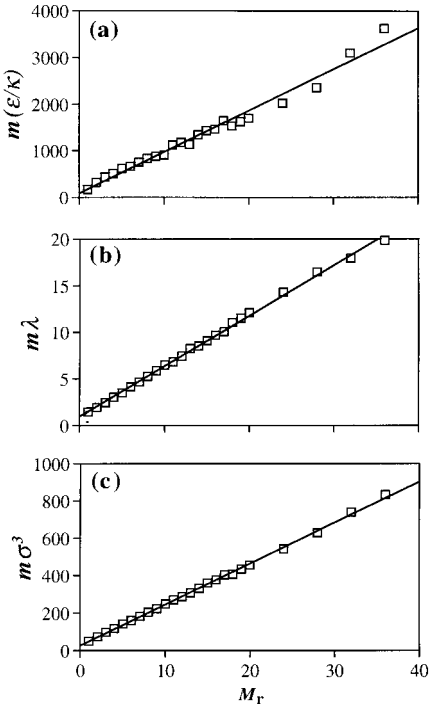

Fig. 4 Dependence of the molecular parameters for each n-alkane on relative molecular mass: (a) ε/k, (b) λ, and (c) σ^3. The solid line is a linear fit through each set of data.

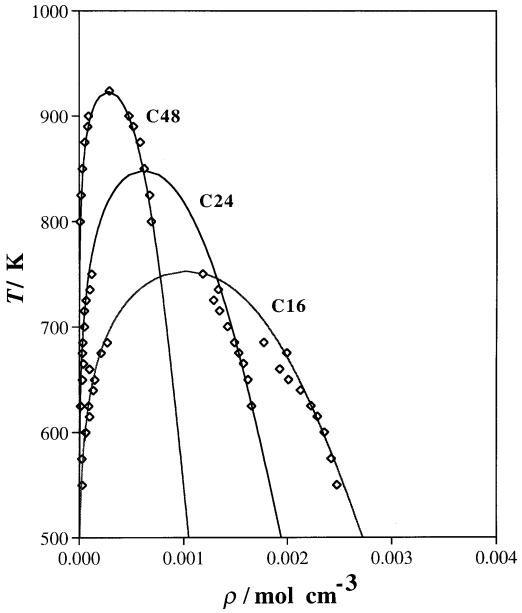

Fig. 5 Comparison of SAFT-VR predictions and computer simulation results of the saturated gas and liquid densities of n-hexadecane ($C_{16}H_{34}$), n-tetracosane ($C_{24}H_{50}$) and n-octatetracontane ($C_{48}H_{98}$). The diamonds are the simulation data of Smit *et al.*[57] and the continuous curves the SAFT-VR predictions.

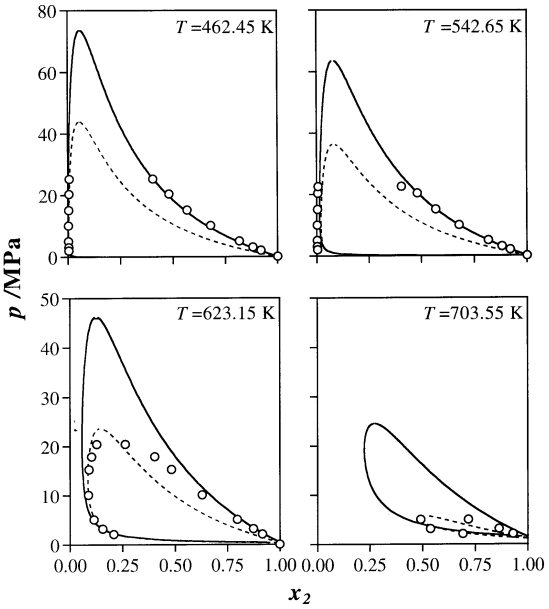

Fig. 6 Four constant temperature p–x slices of the phase diagram for the methane (1) + n-hexadecane ($C_{16}H_{34}$) (2) binary mixture compared with the SAFT-VR prediction. The continuous curves correspond to SAFT-VR predictions with parameters fitted to the vapour pressures and saturated liquid densities of the pure components and the dashed curves with parameters re-scaled to the critical point of each pure component. The circles are the experimental results of Lin *et al.*[40]

the theoretical predictions of SAFT-VR in Fig. 5. For n-hexadecane and n-tetracosane we use the original parameters fitted to vapour pressures and saturated liquid densities (as given in Table 1), while for n-octatetracontane the linear relationships given by eqns. (29)–(31) are used to obtain the parameters. It is encouraging to see excellent agreement between the theoretical results of the SAFT-VR approach and the molecular simulations, especially for n-octatetracontane, the highest molecular weight n-alkane so far examined with the SAFT-VR equation of state.

We have examined a number of binary n-alkane mixtures with the SAFT-VR approach using the MX1b mixing rule[31] as introduced in the previous section. In addition to the pure component parameters the description of phase equilibria in mixtures requires the determination of a number of cross parameters from those of the pure components; as in earlier work on mixtures of the lighter n-alkanes[32,33] the unlike size σ_{12} and energy parameters ε are determined using simple Lorentz–Berthelot combining rules[49] and a simple arithmetic mean rule is used to determine the unlike range parameter λ_{12}. In Fig. 6 we present pressure–composition p–x slices for the methane + n-hexadecane ($C_{16}H_{34}$) binary mixture. The solid lines correspond to SAFT-VR calculations with the original parameters determined from the fit to vapour-pressure and saturated liquid density data, and the dashed curves obtained with parameters re-scaled to the pure component critical points. We can see that with the original parameters the theory accurately reproduces the low pressure behaviour although, as expected, it over-estimates the gas–liquid critical point. On the other hand the results of the SAFT-VR approach using the critical parameters provide a more accurate description of the phase behaviour in the critical region but poorer agreement is obtained at lower pressures, especially at lower temperatures. This comparison highlights the advantage of using parameters re-scaled to the critical points of the pure components in mixture calculations when examining the critical region and in particular critical lines (see for example refs. 32–34).

Additionally we present the full p–T projection of the phase diagram for the n-hexane + n-tetradecane ($C_{14}H_{30}$) binary mixture (Fig. 7). This binary mixture is an example of a simple type I phase diagram according to the classification scheme of Scott and van Konynenburg;[59] a continuous gas–liquid critical line connects the critical points of the two pure components which are completely miscible in all proportions. Type I systems usually comprise non-polar or chemically similar substances, with similar critical properties. For a homologous series like the n-alkanes deviations from type I behaviour are observed when the ratio of the two pure component critical points exceeds a certain limit. In the case of methane + n-alkanes, n-hexane is the first to deviate from type I phase behaviour. For longer n-alkanes the deviations

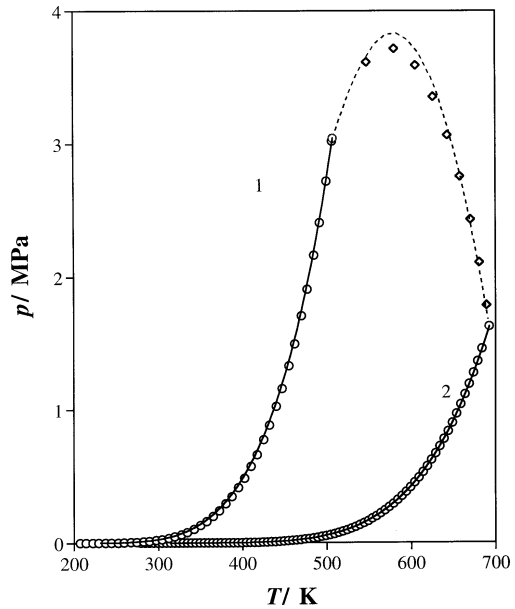

Fig. 7 p–T projection for n-hexane (1) + n-tetradecane ($C_{14}H_{30}$) (2) compared with the SAFT-VR prediction. The continuous curves represent the SAFT-VR vapour pressures for the pure components and the dashed curve the predicted gas–liquid critical line. The circles represent the correlated values for the vapour pressures of the pure components[37] and the diamonds correspond to the experimental gas–liquid critical points.[62]

occur for higher carbon numbers; in the case of ethane a change in phase behaviour is first observed for n-tetradecane ($C_{14}H_{30}$)[60] and for propane with n-dotriacontane ($C_{32}H_{66}$).[61] The theoretical calculations presented in Fig. 7 were obtained from the SAFT-VR equation of state with the critical parameters for methane and tetradecane since we are examining the gas–liquid critical line. As is seen in Fig. 7, the theoretical prediction accurately describes the experimental data,[62] showing only a small deviation at the pressure maximum compared with experiment. We have also examined the phase equilibrium for the methane + n-hexatriacontane ($C_{36}H_{74}$) binary mixture with the SAFT-VR approach,[63] obtaining good agreement between the theoretical predictions and experimental results.[64]

4 Conclusions

We have extended the original work with SAFT-VR to n-alkanes beyond n-octane up to n-hexatriacontane. Parameters for the potential model of each n-alkane are presented and used to determine linear relationships with molecular weight. These provide prescriptions for heavier n-alkanes for which there are no experimental data; the validity of this extrapolation is tested against computer simulation data for n-octatetracontane ($C_{48}H_{98}$) with excellent agreement. Good agreement is seen between SAFT-VR and correlated data for both the vapour pressures and saturated liquid densities, though the inevitable over-prediction in the critical region is observed. We have illustrated that this can be overcome (if an accurate description of the critical point is desired) by re-scaling the parameters to the critical point of each pure component. Additionally we have examined some binary mixtures involving the heavier n-alkane molecules. Simple Lorentz–Berthelot combining rules are used to determine the unlike parameters from those of the pure components. It is particularly gratifying to see that reasonable agreement can be obtained between experimental data and theoretical predictions from the SAFT-VR approach for the longer n-alkane chains without re-fitting cross interaction parameters. The results for n-hexatriacontane and n-octatetracontane are especially encouraging given the large difference in chain length between the two pure components and lead to further work on extending the SAFT-VR approach to polymer systems.

Acknowledgements

CMcC thanks Sheffield University for the award of a UGC Scholarship. We also acknowledge support from the European Commission, the Royal Society, and the Computational and ROPA Initiatives of the EPSRC for the provision of computer hardware.

References

1 M. L. McGlashan, *Pure Appl. Chem.*, 1985, **57**, 89; *J. Chem. Thermodyn.*, 1985, **17**, 301.
2 G. M. Schneider, *Pure Appl. Chem.*, 1991, **63**, 1313.
3 R. D. Gray, J. L. Heidman and R. D. Springer, *Fluid Phase Equilib.*, 1989, **53**, 355.
4 F. Kraft, *Chem. Ber.*, 1882, **15**, 1687; *Chem. Ber.*, 1882, **15**, 1711; *Chem. Ber.*, 1886, **19**, 2218.
5 B. D. Smith and R. Srivastava, *Thermodynamic Data for Pure Compounds*, Elsevier, London, 1986.
6 B. A. Younglove and J. F. Ely, *J. Phys. Chem. Ref. Data*, 1987, **16**, 577.
7 R. C. Reid, J. M. Prausnitz and B. E. Poling, *The Properties of Gases and Liquids*, McGraw-Hill, New York, 4th edn., 1987.
8 M. J. Anselme, M. Gude and A. S. Teja, *Fluid Phase Equilib.*, 1990, **57**, 317.
9 D. R. Stull, *Ind. Eng. Chem.*, 1947, **39**, 517.
10 A. A. Schaerer, C. J. Busso, A. E. Smith and L. B. Skinner, *J. Am. Chem. Soc.*, 1955, **77**, 2017.
11 D. W. Morecroft, *J. Chem. Eng. Data*, 1964, **9**, 488.
12 J. G. Hust and R. E. Schramm, *J. Chem. Eng. Data*, 1976, **21**, 7.
13 R. D. Chirico, A. Nguyen, W. V. Steele, M. Michael Strube and C. Tsonopoulos, *J. Chem. Eng. Data*, 1989, **34**, 149.
14 D. L. Morgan and R. Kobayashi, *Fluid Phase Equilib.*, 1994, **97**, 211.
15 E. D. Nikitin, P. A. Pavlov and P. V. Skripov, *Int. J. Thermophys.*, 1996, **17**, 455.
16 O. Redlich and J. N. S. Kwong, *Chem. Rev.*, 1949, **44**, 233.
17 G. Soave, *Fluid Phase Equilib.*, 1972, **82**, 345.
18 D. Peng and D. B. Robinson, *Ind. Eng. Chem. Fundam.*, 1976, **15**, 59.
19 C. Kim, P. Vimakhand, M. D. Donohue and S. I. Sandler, *AIChE J.*, 1986, **32**, 1726.
20 K. Magoulas and D. Tassios, *Fluid Phase Equilib.*, 1990, **56**, 119.
21 K. A. M. Gasem and R. L. Robinson, *Fluid Phase Equilib.*, 1990, **58**, 13.
22 S. Beret and J. M. Prausnitz, *AIChE J.*, 1975, **21**, 1123; M. D. Donohue and J. M. Prausnitz, *AIChE J.*, 1978, **24**, 549.
23 C. J. Peters, J. de Swaan Arons, J. M. H. Levelt Sengers and J. S. Gallagher *AIChE J.*, 1988, **34**, 834.
24 W. G. Chapman, K. E. Gubbins, G. Jackson and M. Radosz, *Fluid Phase Equilib.*, 1989, **52**, 31.
25 W. G. Chapman, K. E. Gubbins, G. Jackson and M. Radosz, *Ind. Eng. Chem. Res.*, 1990, **29**, 1709.
26 A. Gil-Villegas, A. Galindo, P. J. Whitehead, S. J. Mills, G. Jackson and A. N. Burgess, *J. Chem. Phys.*, 1997, **106**, 4168.
27 S. H. Huang and M. Radosz, *Ind. Eng. Chem. Res.*, 1990, **29**, 2284.
28 S. H. Huang and M. Radosz, *Ind. Eng. Chem. Res.*, 1991, **30**, 1994.
29 F. J. Blas and L. F. Vega, *Ind. Eng. Chem. Res.*, 1998, **37**, 660.
30 J. K. Johnson, J. A. Zwollweg and K. E. Gubbins, *Mol. Phys.*, 1993, **61**, 813.
31 A. Galindo, L. A. Davies, A. Gil-Villegas and G. Jackson and *Mol. Phys.*, 1998, **93**, 241.
32 C. McCabe, A. Galindo, A. Gil-Villegas and G. Jackson *Int. J. Thermophys.*, 1998, **19**, 1511.
33 C. McCabe, A. Gil-Villegas and G. Jackson, *J. Phys. Chem. B*, 1998, **102**, 4183.
34 C. McCabe, A. Galindo, A. Gil-Villegas and G. Jackson, *J. Phys. Chem. B*, 1988, **102**, 8060.
35 A. Galindo, A. Gil-Villegas, P. J. Whitehead and G. Jackson, *J. Chem. Phys. B*, 1998, **102**, 7632.
36 A. Galindo, L. J. Florusse and C. J. Peters, *Fluid Phase Equilib.*, 1999, in the press.
37 T. E. Daubert and R. P. Danner, *Data Compilation Tables of Properties of Pure Compounds*, AIChE, New York, 1985, 1986, 1989; *Design Institute for Physical Property Data*, DIPPR 801 Tables, 1992.
38 M. P. W. M. Rijkers, C. J. Peters and J. de Swaan Arons, *Fluid Phase Equilib.*, 1993, **85**, 335.
39 M. Glaser, C. J. Peters, H. J. Van der Kooi and R. N. Lichtenhaler, *J. Chem. Thermodyn.*, 1985, **17**, 803.
40 H. Lin, H. M. Sebastian and C. Kwnag-Chu, *J. Chem. Eng. Data*, 1980, **25**, 252.
41 G. Jackson and K. E. Gubbins, *Pure Appl. Chem.*, 1989, **61**, 1021.
42 A. Galindo, P. J. Whitehead, G. Jackson and A. N. Burgess, *J. Phys. Chem.*, 1996, **100**, 6781.
43 A. L. Archer, M. D. Amos, G. Jackson and I. A. McLure, *Int. J. Thermophys.*, 1996, **17**, 201.
44 J. P. Hansen and I. N. McDonald, *Theory of Simple Liquids*, Academic Press, London, 2nd edn., 1986.
45 P. J. Leonard, D. Henderson and J. A. Barker, *Trans. Faraday Soc.*, 1970, **66**, 2439.
46 T. Boublík, *J. Chem. Phys.*, 1970, **53**, 471.
47 G. A. Mansoori, N. F. Carnahan, K. E. Starling and T. W. Leland, *J. Chem. Phys.*, 1971, **54**, 1523.
48 N. F. Carnahan and K. E. Starling, *J. Chem. Phys.*, 1969, **51**, 635.
49 J. S. Rowlinson and F. L. Swinton, *Liquids and Liquid Mixtures*, Butterworth Scientific, London, 3rd edn., 1982.
50 C. P. Hicks and C. L. Young, *Chem. Rev.*, 1975, **75**, 119.
51 J. A. Barker and D. Henderson *Rev. Mod. Phys.*, 1975, **48**, 587.
52 J. K. Percus and G. J. Yevick, *Phys. Rev.*, 1958, **110**, 1.
53 W. H. Press, S. A. Teukolsky, W. T. Vetterling and B. P. Flannery, *Numerical Recipes in Fortran*, Cambridge University Press, Cambridge, 1st edn. 1986.
54 J. M. Prausnitz, R. N. Lichtenthaler and E. Gomes de Azevedo, *Molecular Thermodynamics of Fluid-Phase Equilibria*, Prentice-Hall, Englewood Cliffs, NJ, 2nd edn., 1986.
55 A. Z. Panagiotopoulos, *Mol. Simul.*, 1992, **9**, 1; A. Z. Panagiotopoulos and M. R. Stapleton, *Fluid Phase Equilib.*, 1989, **53**, 133.

56 J. I. Siepmann, *Mol. Phys.*, 1990, **70**, 1145; J. I. Siepmann and D. Frenkel, *Mol. Phys.*, 1992, **75**, 59; D. Frenkel, G. C. A. M. Mooij and B. Smit, *J. Phys.: Condens. Matter*, 1992, **4**, 3053.
57 B. Smit, S. Karaborni and J. I. Siepmann, *J. Chem. Phys.*, 1995, **102**, 2126.
58 J. I. Siepmann, S. Karaborni and B. Smit, *J. Am. Chem. Soc.*, 1993, **115**, 6454.
59 R. L. Scott and P. H. van Konynenburg, *Discuss. Faraday Soc.*, 1970, **49**, 87; P. H. van Konynenburg and R. L. Scott, *Philos. Trans. R. Soc. A*, 1980, **298**, 495.
60 C. J. Peters, R. N. Lichtenthaler and J. de Swaan Arons, *Fluid Phase Equilib.*, 1986, **29**, 495.
61 C. J. Peters, H. J. van der Kooi, J. L. de Roo and J. de Swaan Arons, *Fluid Phase Equilib.*, 1989, **51**, 339.
62 S. C. Pak and W. B. Kay, *Ind Eng. Chem. Fundam.*, 1972, **11**, 225.
63 P. Tobaly, C. McCabe and G. Jackson, in preparation.
64 Ph. Marteau, P. Tobaly and G. Lanchec, to be published.

Paper 8/08085B